Research Article

Investigation on Microstructure and Mechanical Characteristics of Sugar Palm Fibre Ash Reinforced LM26 Al-Matrix Composites

Isah Aliyu
Advanced Engineering Materials and Composites Research Centre (AEMC), Department of Mechanical and Manufacturing Engineering, Universiti Putra Malaysia, Selangor, Malaysia
Department of Metallurgical Engineering, Waziri Umaru Federal Polytechnic, Birnin Kebbi, Nigeria

Salit Mohd Sapuan*, Edi Syams Zainudin and Mohd Yusoff Mohamed Zuhri
Advanced Engineering Materials and Composites Research Centre (AEMC), Department of Mechanical and Manufacturing Engineering, Universiti Putra Malaysia, Selangor, Malaysia

Ridwan Yahaya
Science and Technology Research Institute for Defence (STRIDE), Kajang, Selangor, Malaysia

* Corresponding author. E-mail: sapuan@upm.edu.my DOI: 10.14416/j.asep.2023.02.010
Received: 29 November 2022; Revised: 21 December 2022; Accepted: 27 January 2023; Published online: 27 February 2023

Abstract
Aluminium alloy of grade LM26 was used as a matrix and sugar palm fiber ash (SPFA) as reinforcement to investigate its microstructural and mechanical characteristics. Stir casting, a cost-effective method of casting was utilized to fabricate the composites, by altering SPFA from 0 to 10 wt% in 2 wt% increments in an LM26 Al-alloy matrix. The microstructural analysis and phase identification were identified with Scanning Electron Microscopy (SEM) attached to Energy Dispersive Spectroscopy (EDS) and X-ray Diffraction (XRD), respectively. The composites were tested for density, hardness, tensile strength, compression strength, and impact energy according to ASTM. Microstructural images revealed a homogeneous distribution of SPFA in the LM26 Al-alloy matrix. The phases identified in the composites were α-Al, hard SiO_2, Mg_2Si, and Al_5FeSi. The addition of SPFA decreased the composite density and impact energy by 3.85% and 46.68%, respectively. The compression strength and tensile strength of the composites increased by 23.73% and 27.83%, respectively, at an 8 wt% addition of SPFA. However, further addition of up to 10 wt% SPFA showed a decreasing trend in compression and tensile strength. The hardness of the composites increased by 60.80% after a 10 wt% addition of SPFA. These findings showed that synthesized LM26 Al-SPFA composites could be used in the automotive industries for the fabrication of pistons, connecting rods, brake shoes, and other components due to their excellent mechanical characteristics.

Keywords: Density, LM26 Al-alloy, Mechanical properties, Microstructure, Stir casting, Sugar palm fibre

1 Introduction

The growing demand for lightweight materials has attracted the attention of scientists to the use of aluminium matrix composites (AMCs) for specific areas of applications, such as in automotive and aerospace to reduce fuel consumption [1]. Aluminium alloy of grade LM26 (Al-7% Si-1.5% Mg) is gaining recognition and finding application in aerospace and automotive for the manufacturing of wheels, cylinders, pistons, connecting rods, and other engine parts due to excellent physical, mechanical, and casting characteristics, which include low density, excellent high strength-to-weight proportion, better corrosion

resistance, and excellent fluidity. Silicon and magnesium are the major primary alloying elements in LM26 Al-alloy, with a hypoeutectic combination of 7% Si and 0.2–0.6% Mg. This alloy is utilized as a matrix material in the manufacturing of long-lasting composite materials [2].

The Al-matrix has excellent toughness, melting point qualities, corrosion resistance, and excellent thermal and electrical conductivity. Aluminium alloys are the most favored and widely employed base alloys for metal matrix composites in a variety of applications due to their outstanding combination of strength-to-weight ratio, environmental resilience, and stiffness [3]. However, aluminium has low wear resistance; it is mostly lubricated at the boundary and is thermally unstable at high temperatures. The utilization of agro-waste in the form of ash particles as reinforcements improved the hardness, tensile strength, impact strength and increase the wear resistance of most aluminium alloys [4]. Metal matrix composites (MMCs), such as AMCs, have the potential to substitute conventional materials in a wider range of applications, such as medical components, building construction, automotive components, such as connecting rods, pistons, brake discs, and connecting rods, and aerospace components such as wings and fuselages [5].

The most widely employed fabrication techniques employed in the production of AMCs are composite casting [6], powder metallurgy [7], squeeze casting [8], friction stir casting [9], and stir casting [10]. However, stir casting appeared to be the most frequently used among the various fabrication techniques due to its simplicity with adequate flexibility and the most cost-effective in terms of mass production, by utilizing vortex flow due to stirring in the molten metal for uniform dispersion of reinforcements within the matrix [11]. The inadequate wettability between reinforcements and metal matrix limits its application, which is remedied by using double stir casting, the addition of wetting agents and heating the reinforcement prior to its addition into the melt. Achieving sound cast composites requires careful consideration of a number of important production parameters, including melting temperature, die preheating, stirring speed, holding time, stirring time, and stirrer positioning [12].

The synthetic reinforcement materials normally used in aluminium matrix composites are silicon carbide (SiC), alumina (Al_2O_3), boron carbide (B_4C), aluminium nitride (AIN), titanium carbide (TiC), carbon nanotube (CNT), boron nitride (BN), graphite, graphene, etc. The depletion of synthetic reinforcements, coupled with high cost, high weight, and limited supply are major issues faced in most developing countries in the fabrication of AMCs [13]. The reliance on the importation of synthetic materials from overseas, combined with the high cost of foreign exchange, implies that synthetic materials purchased locally are relatively expensive if available. Researchers have shown keen interest in improving the mechanical characteristics of AMC by incorporating inexpensive and readily available agro waste into AMCs [6].

In recent times, the utilization of agro-waste and industrial waste as reinforcement in the manufacturing of AMCs has received the desired attention due to their availability, effortless fabrication process, cost-effectiveness, renewable, and availability, as well as the awareness campaign for preserving the environment and waste management [14]. The utilization of agro wastes as reinforcement material in the manufacturing of AMCs is a viable option with numerous advantages, including the fabrication of low-cost by-products [15], lower costs of aluminium end products [16], improved mechanical properties [17], and lowering of density [18] in comparison to ceramic and synthetic reinforcements like silicon carbide, carbon, and alumina [19]. This has prompted scientists to utilise numerous agro wastes as an alternative to conventional synthetic reinforcements. The application of various agro-waste ash in the form of reinforcement materials in AMCs has been studied [20]. Among the agro wastes used as reinforcements are cotton shells [21], rice husks [22], coconut shells [23], groundnut shells [24], locust bean pods [25], palm kernel shells [26], bamboo leaves [27], and corn cobs [28], while Al 6061 [29], AA 7075 [30], A 2009 [31], AA 2024 [32], ML26 [33], ML6 [34], and Al 6063 [35] are used as matrix.

Abdulrazaq *et al.*, [36] studied the difference in morphology and mechanical characteristics of AMCs strengthened separately with ash from date palm seeds and dolomite, produce via the powder fabrication route. The different reinforcement content used is 2.5, 5, 7.5, and 10 wt%. The microstructures of both fabricated composites revealed uniform dispersion of reinforcements. The AMC reinforced with the ash of date palm seeds ash at 7.5 wt% possesses higher hardness in comparison to the AMC reinforced with

dolomite. The compression strength of date palm seeds ash-reinforced AMC was lower in comparison to the AMC reinforced with dolomite at 7.5 wt% loadings. Balaji *et al.*, [37] investigated the influence of particle size on the mechanical behavior of sugarcane bagasse ash (SCBA) reinforced AMCs produced via stir casting. The amount of reinforcement content of 3, 6, and 9 wt% and sizes ranging from 75–100 μm and 100–150 μm were utilised. The AMCs showed significant improvement in hardness, tensile strength, and impact strength while increasing the content of SCBA. The reinforcement particle size of the range 100–150 μm proves to be stronger in comparison to 75–100 μm.

Dev and Aherwar [33], investigate the mechanical characteristics of piston aluminium alloy (LM26) strengthened with porcelain. The void produced by this composite was found to be reduced while the tensile strength and hardness were improved with the incorporation of porcelain in the LM26 Al-matrix.

Ramachandra and Senthilkumar [38], investigate the characteristics of LM26 hybrid composite strengthened with SiC and B_4C via stir casting. The results show a fairly evenly dispersion of the reinforcement particles with fewer agglomerated SiC and B_4C having a dull and granular morphology. The composite containing 2% SiC and 4% B_4C was found to have better and improved mechanical properties, making it a strong candidate to replace steel in internal combustion piston engines.

Vadghule and Kale [39], investigate the tribological characteristics of an ML26 Al matrix composite strengthened with SiC via stir casting using the Taguchi technique. The findings demonstrated that as the applied load increases, so does the wear rate, and as a result, wear resistance improves as the reinforcing content in the form of SiC increases, as opposed to low levels of SiC reinforcement.

Chakravarthy and Rao [40], investigated the mechanical characteristics of rice husk ash and boron carbide reinforced AMCs produced via stir casting. The incorporation of boron carbide and rice husk ash was in the proportions of 0:0, 0:2.5, 2.5:0, and 5:5. The AMC reinforced with the proportion of reinforcement of 5:5 resulted in higher strength and hardness with homogenous dispersion of the reinforcements.

Sugar palm (*Arenga pinnata*) is a multifunctional species of palm belonging to Palmae family that be used to produce varieties of food and beverages, wood feedstock, and fibres [41]. The fiber can be found all around the trunk of the sugar palm tree. The fiber from sugar palms appears to have many benefits, including affordability, non-toxicity, low density, biodegradability, and high strength [42]. The sugar palm fiber contains refractory materials from the preliminary analysis carried out and is found to be a promising reinforcement material in the fabrication of AMCs.

Therefore, to the best of the author's knowledge, no prior research has been done on the microstructure and mechanical characteristics of sugar palm fiber ash-reinforced LM26 Al-alloy matrix composites. This article is mainly to characterize the physical, hardness, impact energy, tensile strength, compression strength, and morphology of LM26 Al matrix composites reinforced with SPFA sourced from Jempo, Negeri Sembilan, Malaysia. Furthermore, this study revealed the economic value and a new perspective in utilizing of sugar palm fiber as reinforcement in aluminium metal matrix composite production.

2 Materials and Methods

2.1 *Materials*

The elemental constituents of an ingot of aluminium alloy of grade LM26 used as a matrix in this study are shown in Table 1.

Table 1: Elemental constituent of LM26 Al-alloy

Elements	Si	Mg	Cu	Fe	Mn	Zn	Ni	Others	Al
% Mass Fraction	9.70	1.20	2.40	1.10	0.50	0.91	0.83	0.50	Bal.

2.2 *Processing of sugar palm fibre*

The sugar palm fiber used in this work was converted into ash using the procedure described in [43]. The dry sugar palm fibers shown in Figure 1(a) were collected in Jempol town in Negeri Sembilan, Malaysia. The sugar palm fibers were washed in fresh water to remove dust particles before being dried at room temperature in the laboratory for 48 h. The dried SPF was burnt in the open air and left to cool for 24 h. The ash collected was conditioned for 4 h in an electric muffle furnace at 700 °C to decrease carbonaceous

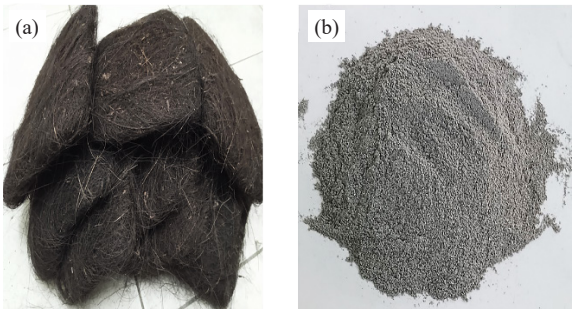

Figure 1: (a) SPF and (b) SPFA.

content and improve the surface oxidation of the SPFA particles. The SPFA was sieved to obtain ash with particles smaller than 75 µm in size. The prepared SPFA, as shown in Figure 1(b), was utilized as reinforcement material. Table 2 displays the chemical constituents of SPFA as ascertained by X-ray Fluorescence (XRF).

Table 2: XRF analysis of sugar palm fiber

Constituents	SiO_2	CaO	Fe_2O_3	Al_2O_3	K_2O	TiO_2	MnO	ZnO	Others
% Mass Fraction	33.49	23.56	16.30	15.10	7.71	1.33	0.54	0.15	1.82

2.3 *Composite production*

Stir casting was used in the fabrication of these composites because it is a low-cost and flexible fabrication route that allows for efficient bonding between the matrix and reinforcement due to adequate stirring. The LM26 Al alloy ingot was cut into smaller pieces and weighed before being placed in a crucible and heated in an electric resistance induction furnace until the entire LM26 Al alloy melted. The molten LM26 Al-alloy was allowed to cool to a semi-solid state inside the furnace at 650 °C. The SPFA was preheated for 2 h at 500 °C to remove moisture and promote wettability with the molten LM26 Al-matrix. SPFA at 2, 4, 6, 8, and 10% were incorporated separately into the semi-cool solid LM26 Al-matrix. Furthermore, 1 wt% hexachloroethane and 1 wt% magnesium were introduced to the semi-solid LM26 Al-alloy to degasify and improve wettability between reinforcements and the matrix, respectively, and the mixture was manually stirred for 5–10 min. Following the heating of the molten composite to 750 °C, a mechanical stirrer

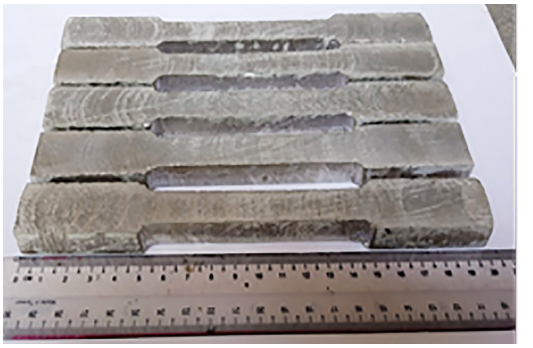

Figure 2: Tensile samples.

was introduced to the melt to complete the secondary stirring process. The stirring was done at a rate of 500 r/min for 10 min for homogeneous dispersion of SPFA particles in LM26 Al-alloy matrix, cast into a sand mould, and tensile strength test samples were produced, as depicted in Figure 2 (ASTM E8 standard) [44]. A similar procedure above was adopted in the production of LM26 Al alloy without adding sugar palm fiber, which serves as a control.

2.4 *X-ray diffraction (XRD) analysis*

X-ray diffractometer (PANalytical X'Pert Pro PW3050/60 Netherlands) equipped with Cu-Kα radiation, wave-length of 1.5406 Å, and scanning speed of 2 °/min in the angle range of $2\theta = (4° – 90°)$ was used to determine the different diffraction peaks, phases, and inter-planar distance in the LM26 Al-matrix alloy and LM26 Al-SPFA composite.

2.5 *Scanning electron microscopy (SEM) analysis*

The morphological details and elemental constituents of various phases in the specimen were analyzed with the assistance of a scanning electron microscope (JSM 6400, JEOL Ltd., Tokyo, Japan) attached to energy dispersive spectroscopy (EDS). Before being placed inside the chamber, the polished test specimens are secured to the specimen holder with double-sided carbon tape.

2.6 *Density determination*

Using the Archimedes principle, the densities of the matrix alloy and the composites produced were

determined. The weight of alloy and composites were measured using a digital electric weighing machine (SER. T0380263, Japan) and then immersed completely in water. The volumes of the samples were calculated by measuring the amount of displaced water. The sample densities were determined using the expression in Equation (1).

$$Density = \frac{Mass}{Volume} \quad (1)$$

2.7 *Tensile and compression strength determination*

A computerized universal testing machine (Instron 3382, USA) of 100 KN with a strain rate of 1.0 min/min was used to measure the tensile and compression strengths of as-cast composite test specimens in accordance with ASTM E-8 and E-9, respectively [44]. The test samples were secured on the lower and upper crossbeam of the grips of the universal testing machine. The tests for ultimate tensile strength and compression strength involved applying a tensile load and a compression load, respectively, until failure occurred on three (3) samples of different compositions. The mean values for tensile and compression strength were calculated and used for the purpose of this study. SEM analysis was utilized to investigate the fracture surfaces of test samples subjected to tensile force.

2.8 *Hardness determination*

Micro hardness test was performed using a digital Mirco-vicker's hardness tester (Model: 401MVD, Germany) in accordance with ASTM E384 [45]. The specimens for the hardness test were machined to 15 mm by 15 mm by 4 mm. Surface flaws were removed by grinding the specimens with 400, 600, 800, and 1000 grit papers followed by polishing. During the test, the specimens were subjected to a load of 1 kg for a dwell time of 15 s, five indentions were taken at various positions on the specimen surface, and the average value represents the hardness values.

2.9 *Hardness determination*

The impact energy of as-cast LM26 Al-matrix/SPFA was assessed using a Charpy impact testing machine (JB: 300, China) of 300 J capacity with a pendulum of striking speed 5 m/s. The specimens were machined into impact test specimens of dimensions of 55 × 10 × 10 mm, with a notch depth of 2 mm, and a radius of tip notch of 0.02 at 45° according to ASTM E23 standard [46]. The impact test was carried out on three test specimens, with readings taken and the average recorded.

3 Results and Discussion

Stir casting was used to successfully fabricate LM26 Al-matrix composite strengthened with SPFA particles. The morphological, density and mechanical characteristics of the LM26 Al-SPFA composites in relation to SPFA content were discussed extensively.

3.1 *Characteristics of SPFA*

Table 2 shows the chemical constituents of the SPFA as determined by XRF. The dominant constituents found in SPFA are SiO_2, CaO, Fe_2O_3, and Al_2O_3. In nature, these refractory oxides (SiO_2, CaO, Fe_2O_3, and Al_2O_3) are known to be exceptionally hard substances [47], [48]. Other oxides discovered in SPFA include K_2O, Ti_2O, MnO, ZnO, and traces of others. Due to the existence of hard substances such as, SiO_2, Al_2O_3, and Fe_2O_3, the SPFA can be used as a reinforcement material.

3.2 *XRD analysis of LM26 Al matrix and LM26 Al/SPFA composite*

The XRD patterns of the LM26 Al alloy and its composite reinforced with SPFA composite are displayed in Figure 3(a) and (b), respectively. The major diffraction peaks of the base matrix are 28.46°, 38.44°, and 44.69°, with inter-planar distances of 3.14 Å, 2.34 Å, and 1.92 Å, respectively, according to the XRD pattern [Figure 3(a)]. The phases found at those peaks are α-Al, Mg_2Si, and Al_5FeSi. The composite major diffraction peaks are 28.37°, 38.38°, and 44.62°, with corresponding inter-planar distances of 3.15 Å, 2.35 Å, and 2.03 Å, and the phases are α-Al, Al_5FeSi, Al_2O_3, SiO_2, and Mg_2Si [Figure 3(b)]. Using these spectrums, the crystalline phases of the composite materials were deduced from the base alloy. The XRD pattern revealed the existence of α-Al, silicon, and magnesium in the LM26 Al-alloy matrix, as well as SPFA particles in the composite.

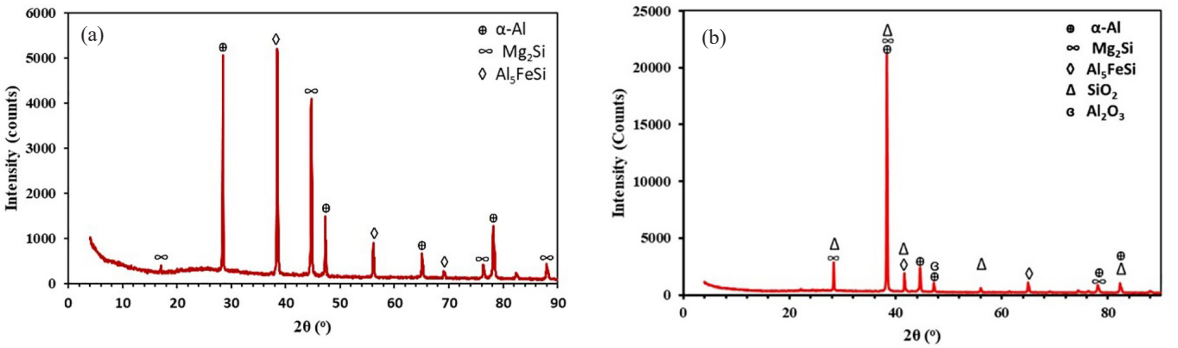

Figure 3: XRD pattern of (a) LM26 Al alloy and (b) LM26 Al/SPFA composite.

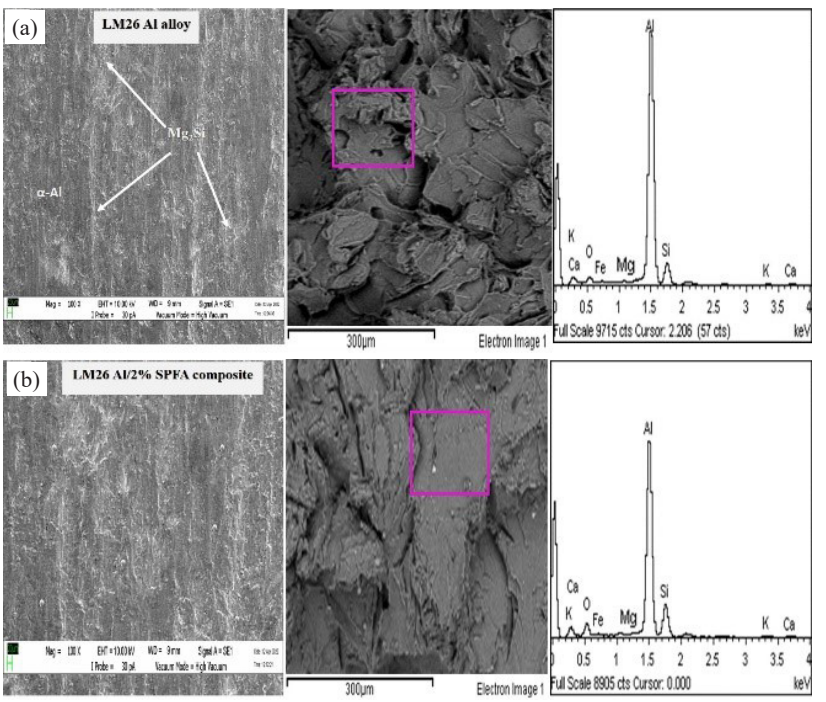

Figure 4: SEM morphology of (a) LM26 Al alloy (b) LM26 Al-2 wt% SPFA composites

3.3 *Morphology of alloy/composite*

The SEM micrographs and EDS spectrums of the LM26 Al matrix alloy and its composites reinforced with SPFA at marked locations are depicted in Figure 4. The existence of eutectic Si and Mg containing Mg_2Si phase in the α-Al matrix is revealed by the microstructure of the unreinforced alloy as evidenced by the EDS spectra [Figure 4(a)]. Figure 4(b)–(e) showed SPFA particles reasonably dispersed in an LM26 Al-alloy matrix, with the distribution proportional to the percentage addition. The uniform distribution could be attributed to the use of appropriate casting parameters such as stirring time, stirring rate, and pre-heating of reinforcements prior to addition, all of which promote wettability. There was no distinct interface between the LM26 Al-alloy and the reinforced SPFA particles, indicating the formation of a strong bond between them [Figures 4(b)–(e)]. The strong interfacial bonding could be attributed to the reinforcement being re-heated prior to its addition, as well as the addition of magnesium, which improved the wettability between the SPFA and LM26 Al alloy.

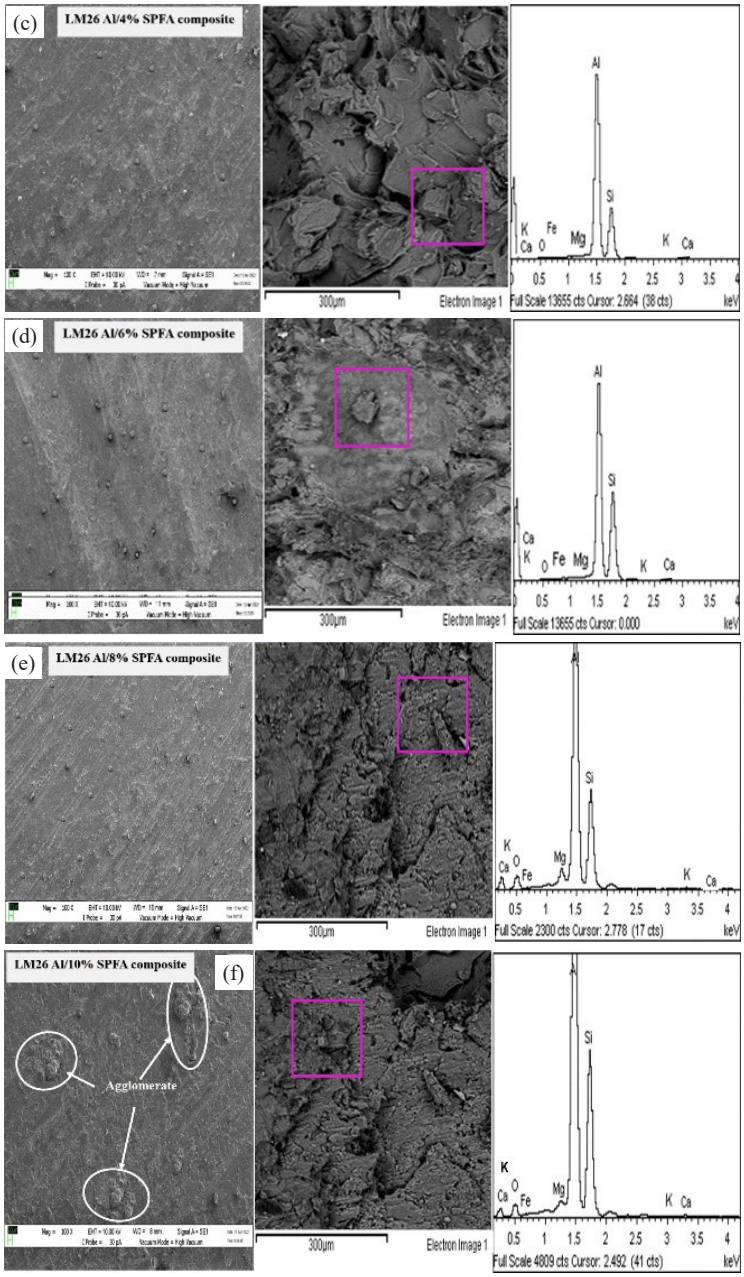

Figure 4: (*Continued*) SEM morphology of (c) LM26 Al-4 wt% SPFA composites (d) LM26 Al-6 wt% SPFA composites (e) LM26 Al-8 wt% SPFA composites (f) LM26 Al-10 wt% SPFA composites.

Consequently, the mechanical characteristics of the produced LM26 Al-SPFA composites are improved. The EDS of the produced LM26 Al-SPFA composites showed the presence of Si, O, C, Mg, Fe, and K, indicating the presence of SPFA, and the peak of Si increases with SPFA addition. In Figure 4(f), there was clustering and formation of agglomerate of SPFA particles on a micro-scale. It is reasonable to conclude that up to 8 wt% SPFA addition into LM26 Al-alloy resulted in good reinforcement dispersion.

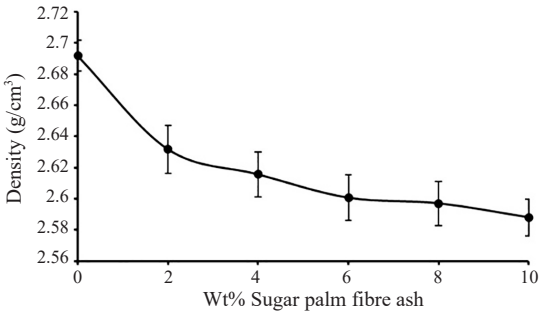

Figure 5: Variation of density with SPFA additions.

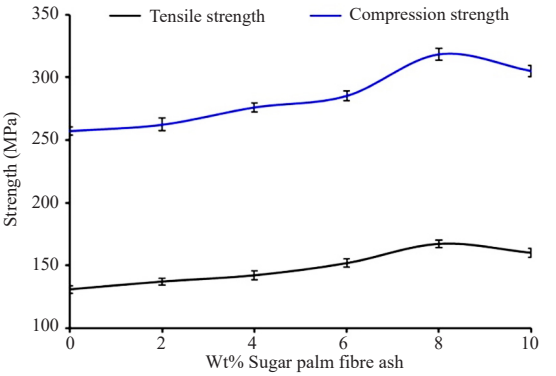

Figure 6: Variation of tensile and compression strength with wt% SPFA addition.

3.4 *Density of the alloy/composites*

The density of LM26 alloy with varying weight percentage additions of SPFA is shown in Figure 5. The densities of the LM26 Al-SPFA composites were observed to be lower in comparison to the base matrix. The density of LM26 Al-alloy composites reinforced with SPFA decreases as the amount of SPFA rises in the matrix as shown in Figure 5. This finding is consistent with the finding of [49], [50]. The density of LM26 Al alloy decreased from 2.69 g/cm^3 to 2.50 g/cm^3 with 10 wt% SPFA addition. The decrease in densities could be attributed to the less dense nature of SPFA, which demonstrated the feasibility of fabricating light-weight Al-alloy matrix composites with SPFA for low-energy consumption in automobile and aerospace applications.

3.5 *Tensile strength and compression strength*

The tensile strength of the LM26 Al alloy-SPFA composite is shown in Figure 6. The tensile strength increased with increased content of SPFA. A pick tensile strength was attained with the incorporation of 8 wt% SPFA, while the least tensile strength was obtained with LM26 Al alloy. The tensile strength was found to increase by 4.78%, 8.59%, 16.04%, and 27.83%, with 2%, 4%, 6%, and 8% SPFA addition, respectively, in comparison to LM26 Al alloy as a control without SPFA. From Figure 6, the results show that SPFA particles strengthen the LM26 Al-matrix composite in terms of mass ratio addition. Tensile strength may have increased as a result of even dispersion of SPFA particles in LM26 Al matrix alloy, as well as excellent interfacial bonding (Figures 7) existing between reinforcement particles and the matrix, which permits load sharing between the LM26 Al alloy matrix and SPFA particle as depicted in SEM micrographs [51], [52]. In addition, the presence of SPFA in the LM26 Al-alloy inhibits dislocation movement. Thereby, increasing the resistance of the composite to plastic deformation and resulting in a high rate of work hardening (Figures 7) [53]. The difference in thermal coefficients between the LM26 Al-alloy matrix and SPFA particles, which led to dislocation density, could also be the reason for the steep rise in strength of the produced composites [54]. The addition of SPFA beyond 8 wt% led to an agglomerate formed in the LM26 Al-alloy matrix. The higher the amount of reinforcement addition, the greater the chances of agglomeration formation, which decreased the hardness of the composite [55]. However, increasing the SPFA content above 8 wt% resulted in a drop of strength from 27.83% to 21.4% at 10 wt% SPFA addition. The formation of SPFA agglomerates in the LM26 Al matrix alloy was the likely cause of the decrease in tensile strength above 8 wt% addition, as shown in Figure 6, due to the weak bond formed between the matrix and the reinforcements [56].

A significant improvement in the compression strength was noticed with increased content of SPFA particles in LM26 Al matrix alloy as depicted in Figure 6. Muralimohan *et al.*, [57] observed a similar trend. The hard ceramic contents present in the SPFA, which include SiO_2, Fe_2O_3, and Al_2O_3 could explain the increase in compression strength up to 8 wt% SPFA addition compared to the LM26 Al matrix alloy. The hard SPFA particles restrict dislocation movement and thus crack propagation by diverting crack growth planes and directions. Similarly, the hard ceramic particles

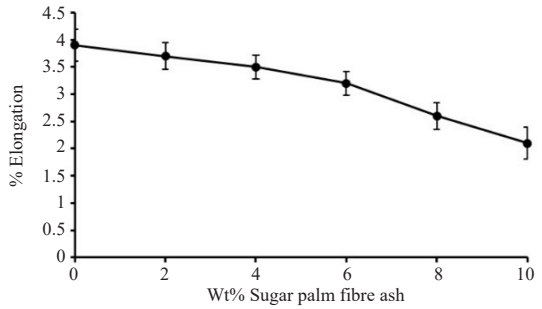

Figure 7: Variation of percentage elongation with wt% SPFA addition.

resist plastic flow, increasing compression strength.

3.6 *Percentage elongation*

The effect of percentage elongation on LM26 Al matrix alloy and its composite reinforced with SPFA is shown in Figure 7. As the weight fraction of SPFA rises, the percentage elongation, which is a function of ductility decreased. Suleiman *et al.*, [58] found a similar trend with melon shell ash employed as reinforcement in the Al-12 % Si matrix. The decrease in ductility could be explained by the addition of more hard and brittle refractory oxides of SPFA into the base matrix.

SEM was utilized to assess the fracture surfaces of tensile test samples. The influence of SPFA content on tensile fracture morphology was thoroughly investigated, as depicted in Figure 8. The micrograph [Figure 8(a)] shows clearly the failure of the LM26 Al alloy is in ductile mode, manifesting as dimples as a result of sharing [Figure 8(a)]. Figure 8(b) showed the presence of microvoids on the surface of the fractured composite, as well as necking and crack formation. The elastic nature of the matrix alloy could attribute to the formation of the neck in the composite. Since the composite containing 2 wt% SPFA is elastic in nature, it deformed by the formation of the neck when the load was applied. It is evident that fine reinforcement particles hinder crack growth in the composites, which are distinguished by the presence of voids. The load applied on the composite is transferred from the LM26 Al matrix to SPFA as reinforcement, thereby increasing the resistance to deformation by plastic flow. This was caused by thermal mismatch due to the high thermal expansion coefficient of the matrix to the low thermal expansion coefficient of the reinforcement material. This thermal mismatch in the composite led to dislocation at the interface. The hard ceramic content in the SPFA introduced into the ductile LM26 Al alloy matrix causes micro-cracks to be formed. As depicted in Figure 8(c), ductile failure in delamination mode was observed in the composite containing 4 wt% SPFA with cracks. According to Figure 8(d), a dimple formed on the fractured surface caused a ductile fracture, which decreased elastic deformation, whereas the cleavage that developed could have been caused by trans-granular grain boundary movement, which led to a brittle fracture. The composite material failed due to the combined action of ductile and brittle fracture, as shown in the SEM micrograph in Figure 8(d). Minor cracks, dimples, and fracture particles of SPFA were noticeable in Figure 8(e), indicating that the composite brittleness had increased. Increasing the concentration of SPFA to 10% wt causes clustering, de-bonding, and crack, which increased the brittleness of the composite, as depicted [Figure 8(f)]. The inclusion of SPFA particles in LM26 Al-alloy matrix composite causes cleavage and delamination, promoting crack initiation and propagation thereby changing the failure mode from ductile to brittle mode. This was also demonstrated in the work of Kumar *et al.* [59].

3.7 *Hardness*

Figure 9 depicts the hardness variation of LM26 Al-alloy with SPFA addition. As depicted in Figure 9, the hardness of LM26 Al alloy increased as SPFA content increased up to 10 wt%. The highest hardness value of 93.62 HV was attained with the addition of 10 wt% SPFA compared to 58.22 HV for the LM26 Al alloy matrix. That is an increment of 60.80% at 10 wt% addition of SPFA. The increase in the trend of hardness with the addition of reinforcement is consistent with the study of Kasagani *et al.* [60]. The hardness of the composites was significantly improved by the presence of hard refractory content of SiO_2, Fe_2O_3, and Al_2O_3 in the SPFA [47]. The uniform dispersion of SPFA in the LM26 Al matrix alloy as depicted in Figures 4(b)–(f) hindered slip movement, which prevents dislocation movement thereby, improving the hardness [13]. The higher the amount of the dispersed SPFA in the matrix, the more strain energy developed at the periphery of the reinforcement, and this led to an improved hard composite [61].

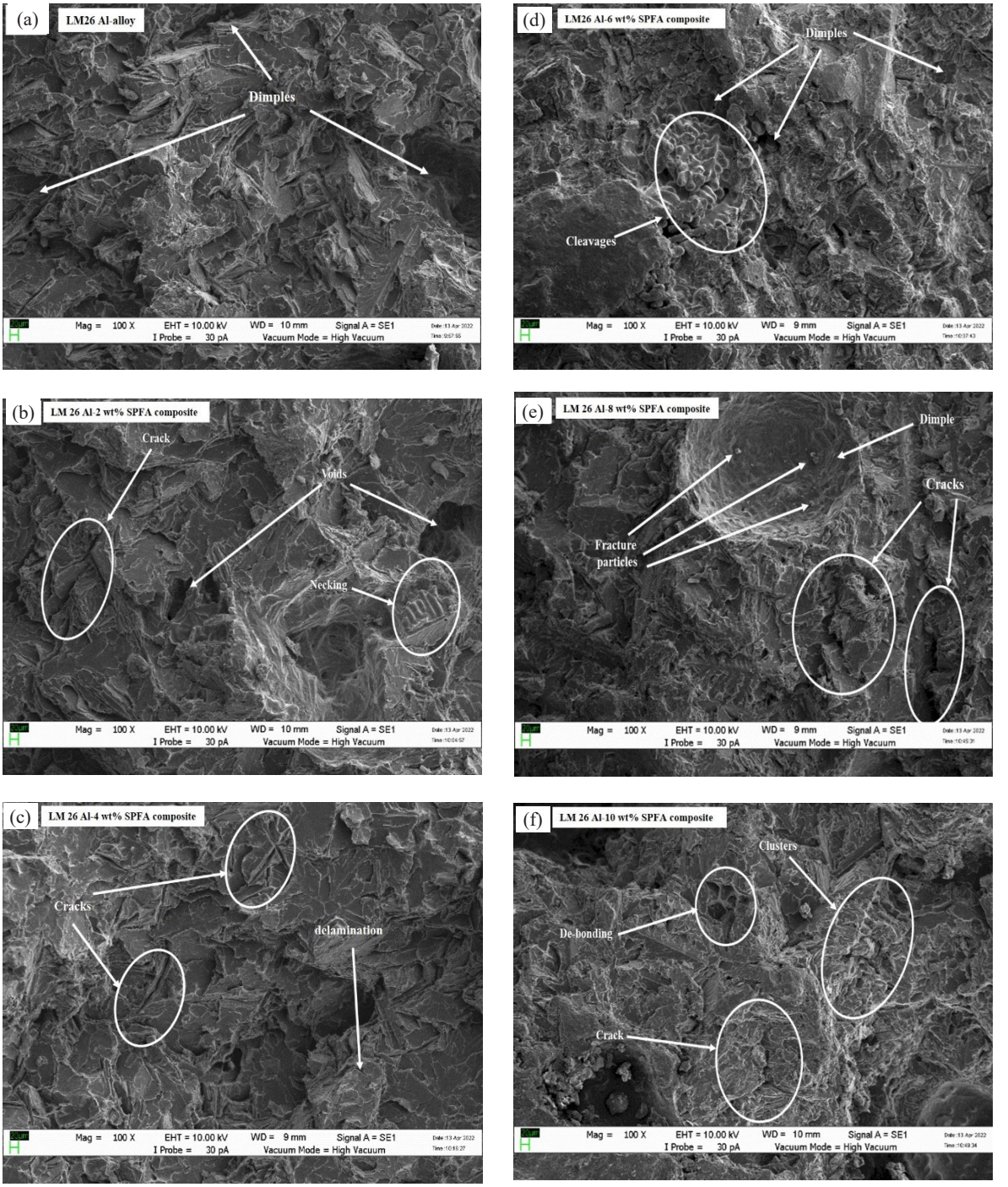

Figure 8: SEM of tensile test fracture surfaces (a) LM26 Al alloy (b) LM26 Al-2 wt% SPFA composite (c) LM26 Al-4 wt% SPFA composite (d) LM26 Al-6 wt% SPFA composite (e) LM26 Al-8 wt% SPFA composite (f) LM26 Al-10 wt% SPFA composite.

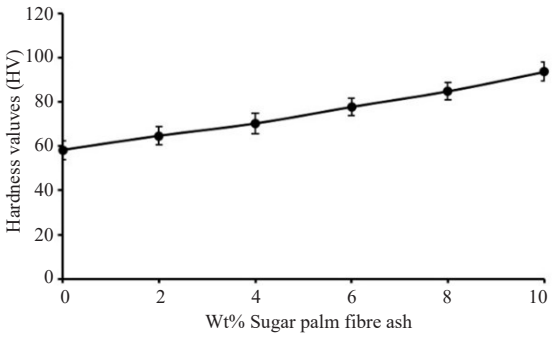

Figure 9: Variation in hardness values with wt% SPFA addition.

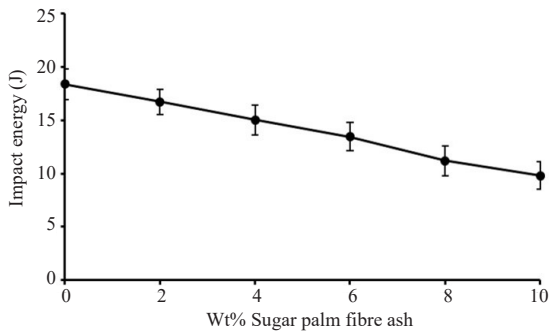

Figure 10: Variation of impact energy with wt% SPFA addition.

3.8 *Impact energy*

The composites were subjected to an impact strength test to determine toughness, which is the ability to withstand shock. The Charpy impact test was used to determine how much energy the composites absorbed in a single strike before braking. Figure 10 depicts the advanced effect of SPFA addition as reinforcement on the impact energy of LM26 Al alloy. The impact energies of virtually all composites were lower compared to the matrix alloy. According to the findings, the impact energy of the composite was observed to have decreased with increased SPFA content. The impact energy of the LM26 Al alloy decreased from 18.38 J to 9.8 J with the addition of 10 wt% SPFA. The SPFA has refractory ceramic content in the form of SiO_2, Fe_2O_3, and Al_2O_3 which are hard and brittle in nature. The addition of the SPFA into the ductile LM26 Al alloy makes it brittle thereby decreasing the impact energy. This is consistent with Aigbodion *et al.* [62] earlier findings.

4 Conclusions

The developed LM26 Al-alloy matrix-SPFA composites have been investigated. The LM26 Al-alloy composites containing different amounts of SPFA particles were successfully fabricated via the stir casting technique. The morphologies of the composites reveal an even distribution of reinforcement in the matrix which is evident in sound casting. The presence of reinforced particles in the composite sample was confirmed by EDS and XRD analysis. The EDS revealed an increase in SPFA content following its addition, which improved tensile strength, compression strength, and hardness while decreasing the density of the composites. The addition of SPFA into LM26 Al-alloy increased tensile strength and compression strength to maximum values of 142.16 MPa and 276.19 MPa, respectively, at 8 wt% SPFA addition while hardness was increased to 84.8HV at 10 wt% SPFA addition. The impact energy, elongation, and density of LM26 Al matrix alloy decreased with the addition of SPFA. The tensile fracture surface morphology revealed the transition from brittle to ductile fracture mode with SPFA addition.

Acknowledgments

The authors are forever grateful to Universiti Putra Malaysia for funding this research through its research grant [GP-IPS/2021/9702700], as well as research facilities and financial support from Waziri Umaru Federal Polytechnic in Birnin Kebbi, Nigeria.

Author Contributions

I A.: investigation, methodology, writing an original draft, research design, data curation, data analysis; M.S.S.: conceptualization, project administration, funding acquisition, research design, reviewing and editing; E.S.Z.: writing-reviewing and editing; M.Y.M.Z.: writing-reviewing and editing; Y.R.: writing-reviewing and editing. The authors have all read and agreed to the published version of the manuscript.

Conflicts of Interest

The authors declare no conflict of interest.

References

[1] J. Grilo, V. H. Carneiro, J. C. Teixeira, and H. Puga, "Manufacturing methodology on casting-based aluminium matrix composites: Systematic review," *Metals*, vol. 11, no. 3, pp. 1–30, 2021, doi: 10.3390/met11030436.

[2] S. Seetharaman, J. Subramanian, R. A. Singh, E. W. L. Wong, S. M. L. Nai, and M. Gupta, "Mechanical properties of sustainable metal matrix composites: A review on the role of green reinforcements and processing methods," *Technologies*, vol. 10, no. 32, pp. 1–27, 2022.

[3] M. H. Kumar, S. M. Rangappa, and S. Siengchin, "A comprehensive review on metal matrix composites for railway applications," *Applied Science Engineering Progrogress*, vol. 15, no. 2, Mar. 2022, doi: 10.14416/j.asep.2022.03.003.

[4] G. Arora and S. Sharma, "A comparative study of aa6351 mono-composites reinforced with synthetic and agro waste reinforcement," *International Journal of Precision Engineering and Manufacturing*, vol. 19, no. 4, pp. 631–638, Apr. 2018, doi: 10.1007/s12541-018-0076-1.

[5] M. Ramasamy, A. A. Daniel, and M. Nithya, "Investigation on surface roughness of aluminium (Al7050/TiC/BN) hybrid metal matrix," *Materials Today: Proceedings*, vol. 46, pp. 852–856, 2021, doi: 10.1016/j.matpr.2020.12.852.

[6] A. H. Khan, S. A. S. Ahmad, F. Umar, U Noor, R. M. Gul, K. Giasin, and M. Aamir, "Investigating the microstructural and mechanical properties of novel ternary reinforced AA7075 hybrid metal matrix composite," *Materials*, vol. 15, no. 5303, pp. 1–18, 2022.

[7] M. B. N. Shaikh, S. Arif, T. Aziz, A. Waseem, M. A. N. Shaikh, and M. Ali, "Microstructural, mechanical and tribological behaviour of powder metallurgy processed SiC and RHA reinforced Al-based composites," *Surfaces and Interfaces*, vol. 15, no. May 2018, pp. 166–179, 2019, doi: 10.1016/j.surfin.2019.03.002.

[8] N. S. Kumar, "Fabrication and characterization of Al7075 / RHA /Mica composite by squeeze casting," *Materials Today: Proceedings*, vol. 37, no. 2, pp. 750–753, 2020, doi: 10.1016/j.matpr.2020.05.769.

[9] O. M. Ikumapayi, E. T. Akinlabi, J. D. Majumdar, O. P. Oladijo, and S. A. Akinlabi, "Influence of wood fly ash reinforcement on the wear behaviour of friction stir processed aluminium-based surface matrix composite," *Proceedings of the International Conference on Industrial Engineering Operations Management*, 2019, vol. l, pp. 966–977.

[10] S. R. Prabhu, A. K. Shettigar, M. A. Herbert, and S. S. Rao, "Microstructure and mechanical properties of rutile-reinforced AA6061 matrix composites produced via stir casting process," *Transaction Nonferrous Metals Society of China*, vol. 29, no. 11, pp. 2229–2236, 2019, doi: 10.1016/S1003-6326(19)65152-6.

[11] H. I. Akbar, E. Surojo, D. Ariawan, A. R. Prabowo, and F. Imanullah, "Fabrication of AA6061-sea sand composite and analysis of its properties," *Heliyon*, vol. 7, no. 8, Aug. 2021, doi: 10.1016/j.heliyon.2021.e07770.

[12] R. Manikandan, T. V. Arjunan, and A. R. Nath O. P, "Studies on micro structural characteristics, mechanical and tribological behaviours of boron carbide and cow dung ash reinforced aluminium (Al 7075) hybrid metal matrix composite," *Composite Part B: Engineering*, vol. 183, no. 2019, Feb. 2020, doi: 10.1016/j.compositesb.2019.107668.

[13] O. M. Ikumapayi, S. A. Afolalu, O. P. Bodunde, C. P. Ugwuoke, H. A. Benjamin, and E. T. Akinlabi, "Efficacy of heat treatment on the material properties of aluminium alloy matrix composite impregnated with silver nano particle/calcium carbonate Al –AgNp/$CaCO_3$," *International Journal of Advanced Technology Engineering Exploration*, vol. 9, no. 89, Apr. 2022, doi: 10.19101/IJATEE.2021.874829.

[14] B. U. Odoni, F. Odikpo, N. C. Chinasa, and R. O. Akaluzia, "Experimental analysis, predictive modelling and optimization of some physical and mechanical properties of aluminium 6063 alloy based composites reinforced with corn cob ash," *Journal of Materials and Engineering Structures*, vol. 7, pp. 451–465, 2020.

[15] C. H. Gireesh, K. G. D. Prasad, K. Ramji, and P. V. Vinay, "Mechanical characterization of aluminium metal matrix composite reinforced with aloe vera powder," *Materials Today: Proceedings*, vol. 5, no. 2, pp. 3289–3297, 2018, doi: 10.1016/j.matpr.2017.11.571.

[16] S. P. Dwivedi, M. Maurya, N. K. Maurya, A. K. Srivastava, S. Sharma, and A. Saxena, "Utilization of groundnut shell as reinforcement in development of aluminum based composite to reduce environment pollution: A review," *Evergreen*, vol. 7, no. 1, pp. 15–25, 2020, doi: 10.5109/2740937.

[17] C. S. Shyn, R. Rajesh, and M. D. Anand, "Review of aluminium 6061 metal matrix composites fabricated using stir casting method and applications," *AIP Conference Proceedings*, vol. 2317, 2021 , doi: 10.1063/5.0036169.

[18] A. M. Razzaq, D. L. Majid, U. M. Basheer, and H. S. S. Aljibori, "Research summary on the processing, mechanical and tribological properties of aluminium matrix composites as effected by fly ash reinforcement," *Crystals*, vol. 11, no. 1212, pp. 1–20, 2021.

[19] N. K. Maurya, M. Maurya, A. K. Srivastava, S. P. Dwivedi, A. Kumar, and S. Chauhan, "Investigation of mechanical properties of Al 6061/SiC composite prepared through stir casting technique," *Materials Today: Proceedings*, vol. 25, pp. 755–758, 2019, doi: 10.1016/j.matpr.2019.09.003.

[20] V. Veeranaath, S. Sengupta, and R. Joseph, "Analysis of the effect of processing constraints and reinforcement content in properties of aluminum hybrid composites," *Materials Today: Proceedings*, vol. 68, pp. 2115–2124, 2022, doi: 10.1016/j.matpr.2022.08.396.

[21] P. Harish, V. M. Srikanth, P. R. Babu, and M. R. C. Sastry, "Characterization of mechanical and tribological properties of aluminium alloy based hybrid composites reinforced with cotton shell ash and silicon carbide," *International Journal Latest Engineering Science*, vol. 2, no. 4, pp. 1–15, 2019.

[22] O. Olaniran, O. Uwaifo, E. Bamidele, and B. Olaniran, "An investigation of the mechanical properties of organic silica, bamboo leaf ash and rice husk reinforced aluminium hybrid composite," *Material Science and Engineering International Journal*, vol. 3, no. 4, 2019, doi: 10.15406/mseij.2019.03.00103.

[23] S. G. Datau, M. A. Bawa, J. S. Jatau, M. H. Muhammad, and A. S. Bello, "The potentials of kyanite particles and coconut shell ash as strengthener in aluminum alloy composite for automobile brake disc," *Journal Minerals and Materials Characterization and Engineering*, vol. 8, no. 3, pp. 84–96, 2020, doi: 10.4236/jmmce.2020.83006.

[24] J. Singh, N. M. Suri, and A. Verma, "Affect of mechanical properties on groundnut shell ash reinforced Al 6063," *International Journal for Technological Research in Engineering*, vol. 2, no. 11, pp. 2619–2623, 2015.

[25] M. A. Bawa, O. B. Umaru, B. T. Abur, I. Salako, and J. S. Jatau, "Effect of locust bean pod ash on the hardness and wear rate of heat treated a356 alloy metal matrix composite for production of automobile brake rotor," *International Journal of Research Publications*, vol. 57, no. 1, pp. 36–43, Jul. 2020, doi: 10.47119/IJRP100571720201325.

[26] I. C. Ezema, V. S. Aigbodion, E. G. Okonkwo, and C. S. Obayi, "Fatigue properties of value-added composite from Al-Si-Mg/palm kernel shell ash nanoparticles," *International Journal of Advanced Manufacturing Technology*, vol. 107, no. 7–8, pp. 3247–3257, 2020, doi: 10.1007/s00170-020-05268-z.

[27] N. S. Ebenezer, B. Vinod, and H. S. Jagadesh, "Corrosion Behaviour of bamboo leaf ash-reinforced nickel surface-deposited aluminium metal matrix composites," *Journal of Bio- and Tribo-Corrosion*, vol. 7, no. 2, pp. 1–7, 2021, doi: 10.1007/s40735-021-00510-x.

[28] K. O. Babaremu and O. O. Joseph, "Experimental study of corncob and cow horn AA6063 reinforced composite for improved electrical conductivity," *Journal of Physics: Conference Series*, vol. 1378, no. 4, 2019, doi: 10.1088/1742-6596/1378/4/042048.

[29] N. E. Udoye, O. S. I. Fayomi, and A. O. Inegbenebor, "Fractography and tensile properties of AA6061 aluminium alloy/rice husk ash silicon nanocomposite," *International Journal of Chemical Engineering*, vol. 2020, pp. 1–8, 2020, doi: 10.1155/2020/8818224.

[30] A. Sharma and P. M. Mishra, "Effects of various reinforcements on mechanical behavior of AA7075 hybrid composites," *Materials Today: Proceedings*, vol. 18, pp. 5258–5263, 2019, doi: 10.1016/j.matpr.2019.07.526.

[31] X. Guo, Q. Guo, J. Nie, Z. Liu, Z. Li, G. Fan,

D. Xiong, Y Su, J. Fan, and D. Zhang, "Particle size effect on the interfacial properties of SiC particle-reinforced Al-Cu-Mg composites," *Materials Science and Engineering A*, vol. 711, pp. 643–649, 2018, doi: 10.1016/j.msea.2017.11.068.

[32] S. Jannet, R. Raja, S. R. Ruban, S. Khosla, U. Sasikumar, N. B. Sai, and P. M. Teja, "Effect of egg shell powder on the mechanical and microstructure properties of AA 2024 metal matrix composite," *Materials Today: Proceedings*, vol. 44, pp. 135–140, 2021, doi: 10.1016/j.matpr.2020.08.546.

[33] S. Dev and A. Aherwar, "Study of physico-mechanical properties of procelain filled aluminium LM26 alloy for piston material," *International Journal of Mechanical and Production Engineering*, vol. 4, no. 9, pp. 38–41, 2016.

[34] P. Mishra, P. Mishra, and R. S. Rana, "Effect of rice husk ash reinforcements on mechanical properties of aluminium alloy (LM6) matrix composites," *Materials Today: Proceedings*, vol. 5, no. 2, pp. 6018–6022, 2018, doi: 10.1016/j.matpr.2017.12.205.

[35] P. V. Reddy, P. R. Prasad, D. M. Krishnudu, and E. V. Goud, "An investigation on mechanical and wear characteristics of Al 6063/TiC metal matrix composites using RSM," *Journal of Bio- and Tribo-Corrosion*, vol. 5, no. 4, pp. 1–10, 2019, doi: 10.1007/s40735-019-0282-0.

[36] A. A. Abdulrazaq, S. R. Ahmed, and F. M. Mahdi, "Agricultural waste and natural dolomite for green production of aluminum composites," *Cleaner Engineering and Technology*, vol. 11, Dec. 2022, doi: 10.1016/j.clet.2022.100565.

[37] A. Balaji, K. Gomathi, U. S. Naveen Rajan, J. Mithil, A. Vinunath, and R. C. Vagish, "Effect of particle size on mechanical behavior of sugarcane bagasse ash reinforced AlSi10Mg alloy," *Materials Today: Proceedings*, vol. 66, pp. 1276–1283, 2022, doi: 10.1016/j.matpr.2022.05.126.

[38] K. R. Raju and G. Senthilkumar, "Investigation on properties of LM26 hybrid composite material with ceramic reinforcements," *Mateials Today: Proceedins*, vol. 45, pp. 8086–8093, 2021, doi: 10.1016/j.matpr.2021.01.286.

[39] A. Y. Vadghule and P. V. C. Kale, "Tribological evaluation of LM26 aluminum metal matrix composites," *International Research Journal of Engineering Technology (IRJET)*, vol. 5, no. 6, pp. 2553–2558, 2018.

[40] M. P. Chakravarthy and D. S. Rao, "Proceedings Evaluation of mechanical properties of aluminium alloy (AA6082) reinforced with Rice husk ash (RHA) and Boron carbide (B_4C) hybrid metal matrix composites using stir casting method," *Materials Today: Proceedings*, vol. 66, pp. 580–586, 2022.

[41] M. L. Sanyang, S. M. Sapuan, M. Jawaid, M. R. Ishak, and J. Sahari, "Recent developments in sugar palm (*Arenga pinnata*) based biocomposites and their potential industrial applications: A review," *Renewable Sustainable Energy Reviews*, vol. 54, pp. 533–549, Feb. 2016, doi: 10.1016/j.rser.2015.10.037.

[42] R. A. Ilyas, S. M. Sapuan, A. Atiqah, R. Ibrahim, H. Abral, M. R. Ishak, E. S. Zainudin, N. M. Nurazzi. M. S. N. Atikah, M. N. M. Ansari, M. R. M. Asyral, A. B. M. Supian, and H. Ya, "Sugar palm (*Arenga pinnata* [*Wurmb*.] *Merr*) starch films containing sugar palm nanofibrillated cellulose as reinforcement: Water barrier properties," *Polymer Composites*, vol. 41, no. 2, pp. 459–467, Feb. 2020, doi: 10.1002/pc.25379.

[43] S. S. Panda, A. K. Senapati, and P. S. Rao, "Effect of particle size on properties of industrial and agro waste-reinforced aluminum-matrix composite," *The Journal of The Minerals, Metals & Materials Society*, vol. 73, no. 7, pp. 2096–2103, 2021, doi: 10.1007/s11837-021-04700-3.

[44] *Standard Test Methods for Tension Testing of Metallic Materials*, ASTM E8/E8M:2013, 2013.

[45] *Standard Test Method for Microindentation Hardness of Materials*, ASTM E 384:2005, 2005.

[46] *Standard Test Methods for Notched Bar Impact Testing of Metallic Materials*, ASTM E 23:2018, 2018.

[47] P. P. Ikubanni, M. Oki, A. A. Adeleke, A. A. Adediran, and O. S. Adesina, "Influence of temperature on the chemical compositions and microstructural changes of ash formed from palm kernel shell," *Results in Engineering*, vol. 8, 2020, doi: 10.1016/j.rineng.2020.100173.

[48] C. U. Atuanya, A. O. A. Ibhadode, and I. M. Dagwa, "Effects of breadfruit seed hull ash on the microstructures and properties of Al-Si-Fe alloy/

breadfruit seed hull ash particulate composites," *Results in Physics*, vol. 2, pp. 142–149, 2012, doi: 10.1016/j.rinp.2012.09.003.

[49] N. K. Chandla, Yashpal, S. Kant, M. M. Goud, and C. S. Jawalkar, "Experimental analysis and mechanical characterization of Al 6061/ alumina/bagasse ash hybrid reinforced metal matrix composite using vacuum-assisted stir casting method," *Journal of Composite Materials*, vol. 54, no. 27, pp. 4283–4297, 2020, doi: 10.1177/0021998320929417.

[50] K. S. Madhu, C. V Venkatesh, B. N. Sharath, and S. Karthik, "Characterization and evaluation of mechanical properties of Al-Zn based hybrid metal matrix composites," *Applied Science Engineering Progrogress*, vol. 16, no. 1, pp. 1–13, 2023.

[51] S. O. Akinwamide, O. J. Akinribide, and P. A. Olubambi, "Microstructural evolution, mechanical and nanoindentation studies of stir cast binary and ternary aluminium based composites," *Journal of Alloys and Compound*, vol. 850, 2021, doi: 10.1016/j.jallcom.2020.156586.

[52] A. Lakshmikanthan, T. R. Prabhu, U. S. Babu, P. G. Koppad, M. Gupta, M. Krishna, and S. Bontha, "The effect of heat treatment on the mechanical and tribological properties of dual size SiC reinforced A357 matrix composites," *Journal of Materials Research and Technology*, vol. 9, no. 3, pp. 6434–6452, 2020, doi: 10.1016/ j.jmrt.2020.04.027.

[53] M. Udo, P. Babalola, S. Afolalu, S. Ongbali, F. Apeh, and O. Olayiwola-Busari, "Effect of sic reinforcement on mechanical and electrical properties of magnesium-aluminium (Mg-Al) alloy matrix composite," *IOP Conference Series Materials Science and Engineering*, vol. 1107, no. 1, Apr. 2021, doi: 10.1088/1757-899X/1107/ 1/012207.

[54] A. K. Yadav, K. M. Pandey, and A. Dey, "Aluminium metal matrix composite with rice husk as reinforcement: A review," *Materials Today: Proceedings*, vol. 5, no. 9, pp. 20130–20137, 2018, doi: 10.1016/j.matpr.2018.06.381.

[55] Y. Afkham, R. A. Khosroshahi, S. Rahimpour, C. Aavani, D. Brabazon, and R. T. Mousavian, "Enhanced mechanical properties of in situ aluminium matrix composites reinforced by alumina nanoparticles," *Archives of Civil and Mechanical Engineering*, vol. 18, no. 1, pp. 215–226, Jan. 2018, doi: 10.1016/j.acme.2017.06.011.

[56] M. Satheesh and M. Pugazhvadivu, "Investigation on physical and mechanical properties of Al6061-Silicon Carbide (SiC)/Coconut shell ash (CSA) hybrid composites," *Physica B: Condensed Matter*, vol. 572, pp. 70–75, Nov. 2019, doi: 10.1016/j.physb.2019.07.058.

[57] R. Muralimohan, U. N. Kempaiah, and Seenappa, "Influence of rice husk ash and B_4C on mechanical properties of ADC 12 alloy hybrid composites," *Materials Today: Proceedings*, vol. 5, no. 11, pp. 25562–25569, 2018, doi: 10.1016/j.matpr. 2018.10.363.

[58] I. Y. Suleiman, S. A. Salihu, and T. A. Mohammed, "Investigation of mechanical, microstructure, and wear behaviors of Al-12% Si/reinforced with melon shell ash particulates," *International Journal of Advanced Manufacturing Technology*, vol. 97, pp. 4137–4144, 2018.

[59] K. R. Kumar, T. Pridhar, and V. S. S. Balaji, "Mechanical properties and characterization of zirconium oxide (ZrO_2) and coconut shell ash(CSA) reinforced aluminium (Al 6082) matrix hybrid composite," *Journal of Alloys Compounds*, vol. 765, pp. 171–179, 2018, doi: 10.1016/j.jallcom.2018.06.177.

[60] S. Kasagani, P. N. Bellamkonda, and S. Sudabathula, "Wear and friction behaviour of coconut shell ash reinforced Aa-7075 metal," *International Journal of Research*, vol. 8, no. 477, pp. 477–485, 2020.

[61] B. C. Kandpal, J. Kumar, and H. Singh, "Fabrication and characterisation of Al_2O_3/aluminium alloy 6061 composites fabricated by Stir casting," *Materials Today: Proceedings*, vol. 4, no. 2, pp. 2783–2792, 2017, doi: 10.1016/j.matpr. 2017.02.157.

[62] V. S. Aigbodion, S. B. Hassan, and J. E. Oghenevweta, "Microstructural analysis and properties of Al-Cu-Mg/bagasse ash particulate composites," *Journal of Alloys Compou*nds, vol. 497, no. 1–2, pp. 188–194, 2010, doi: 10.1016/j.jallcom. 2010.02.190.